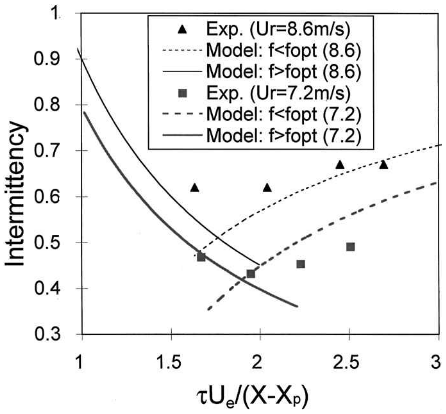

Fig. 4 Measured time-average intermittency factors of the boundary layer forced at different periods compared with calculations based on all the terms of Eq. (1) (- - - -) and Eq. (1a) (——) for $U_r = 7.2$ m/s, $X_p = 0.3$ m, $X_{tr} = 1.25$ m, $X = 1.5$ m, $Z = Z_p$, and for $U_r = 8.6$ m/s, $X_p = 0.5$ m, $X_{tr} = 0.85$ m, $Z_p = 0.04$ and 0.08 m, and $Z = 0.04$ m.

Conclusions

A train of turbulent strips generated upstream of a steady flow transition region can reduce the average intermittency to about half its value downstream of the steady transition location. Periods of laminar flow were maintained in an otherwise turbulent environment. However, the calmed region is eroded inside the turbulent boundary layer, probably by the generation of new spots inside it. Simple kinematic modeling of the described phenomena is capable of reproducing most of the measured events that are relevant to transition delay in turbomachines. Further experiments are needed to explore the creation of new spots inside the calmed region.

Acknowledgments

This work was compiled while the first author held a National Research Council/NASA Langley Research Center research associateship. The experiments were performed at Tel-Aviv University. The helpful suggestions by Bart Singer, NASA Langley Research Center, are appreciated.

References

[1]Pfeil, H., Herbst, R., and Schröder, T., "Investigation of Laminar-Turbulent Transition of Boundary-Layers Disturbed by Wakes," American Society of Mechanical Engineers, ASME Paper 82-GT-124, June 1982.

[2]Halstead, D. E., Wisler, D. C., Okiishi, T. H., Walker, G. J., Hodson, H. P., and Shin, H. W., "Boundary-Layer Development in Axial Compressors and Turbines. Part 1 of 4: Composite Picture," *Journal of Turbomachinery*, Vol. 119, No. 1, 1997, pp. 114–127.

[3]Schubauer, G. B., and Klebanoff, P. S., "Contributions to the Mechanics of Boundary-Layer Transition," NACA Rept. 1289, Feb. 1956.

[4]Cumpsty, N. A., Dong, Y., and Li, Y. S., "Compressor Blade Boundary Layers in the Presence of Wakes," American Society of Mechanical Engineers, ASME Paper 95-GT-443, June 1995.

[5]Schulte, V. S., and Hodson, H. P., "Unsteady Wake Induced Boundary-Layer Transition in Highly Loaded LP Turbines," American Society of Mechanical Engineers, ASME Paper 96-GT-486, June 1996.

[6]Seifert, A., and Wygnanski, I. J., "On Turbulent Spots in a Laminar Boundary-Layer Subjected to a Self-Similar Adverse Pressure Gradient," *Journal of Fluid Mechanics*, Vol. 296, Aug. 1995, pp. 185–209.

[7]Seifert, A., "Spot Calming Effect on Boundary-Layer Transition," *1997 Minnowbrook II Workshop on Boundary Layer Transition in Turbomachines*, edited by J. E. LaGraff and D. E. Ashpiz, NASA CP-1998-206958, 1998, pp. 99–110.

[8]Glezer, A., Katz, Y., and Wygnanski, I., "On the Breakdown of the Wave Packet Trailing Turbulent Spots in a Laminar Boundary-Layer," *Journal of Fluid Mechanics*, Vol. 198, 1989, pp. 1–26.

[9]Gostelow, J. P., Walker, G. J., Solomon, W. J., Hong, G., and Melwani, N., "Investigation of the Calmed Region Behind a Turbulent Spot," American Society of Mechanical Engineers, ASME Paper 96-GT-489, June 1996.

[10]Hodson, H. P., "Modelling Unsteady Transition and Its Effects on Profile Loss," *Propulsion and Energetics Panel 74th(A) Specialists' Meeting*, CP-486, AGARD, 1989.

P. R. Bandyopadhyay
Associate Editor

Grid Adaption for Shock/Turbulent Boundary-Layer Interaction

N. Qin* and Y. Zhu†
Cranfield University, Bedford,
England MK43 0AL, United Kingdom

Introduction

FOR shock/turbulent boundary-layer interaction problems common to aeronautical applications, the severe adverse pressure gradient at the foot of the shock wave makes the turbulence modeling a very challenging task. While concentrating on the physical modeling, one should also be aware of numerical errors introduced from the discretization of the physical modeling and from the computational solution of the discretized equations. The variation of solutions for different grids or different numerical schemes can be as significant as that from different turbulence models. The merit of different models not only depends on the appropriate level of the physical modeling but also on the numerical accuracy and robustness in the computation. Both the discretization scheme and the computational grid play important roles in the numerical accuracy. Ideally one should choose discretization schemes that produce less numerical dissipation so that the numerical results will be less sensitive to the grid used. Furthermore, turbulence models, their implementation, and the related boundary conditions may also introduce a strong dependency on the grid quality. For a given physical model and a given discretization scheme, grid sensitivity study is a very useful way to eliminate numerical uncertainties in computational simulations. However, for multidimensional problems, the process of doubling grid points in each direction, a common practice for grid sensitivity studies for a structured grid approach, can soon exhaust the resources of an available computer system.

Based on equidistribution algorithms, a structured grid adaption[1,2] aims to distribute the numerical errors more evenly by redistributing the grid points along a grid line according to solution activities. Here an assumption has been made that the solution activity is properly measured to reflect the errors between the discretized computational solution and the solution of the governing partial differential equations. For the present study, a structured anisotropic grid adaption approach is adopted to resolve the λ-shock wave, the turbulent boundary layer, and the strong shock/boundary-layer interaction involving boundary-layer separation. The effects of the grid adaption on the flowfield solution, in particular, the turbulent boundary-layer profiles, are studied. This provides a more reasonable and efficient means to carry out grid sensitivity studies through which we can make a fair judgement of a particular turbulence model.

Methodology

The governing equations are the two-dimensional Reynolds averaged Navier–Stokes equations strongly coupled with the two turbulence equations. The shear stress transport (SST) model[3] has exhibited a better capability in dealing with the strong adverse pressure gradient that occurs in shock/boundary-layer interaction problems among a number of two-equation models tested.[4]

The convective numerical flux at the cell interface is evaluated using the Osher approximate Riemann solver with a MUSCL interpolation for a higher-order accuracy. The viscous fluxes and the turbulent source terms are discretized by using central differences through the use of Gauss's theorem. The time discretization

Presented as Paper 98-0227 at the AIAA 36th Aerospace Sciences Meeting, Reno, NV, 12–15 January 1998; received 30 March 1998; revision received 12 April 1999; accepted for publication 28 April 1999.

*Senior Lecturer, College of Aeronautics; N.Qin@cranfield.ac.uk. Senior Member AIAA.

†Ph.D. Student, College of Aeronautics.

is achieved through an explicit multistage Runge–Kutta method with local time stepping.

A structured grid movement strategy[1,2] is employed in our adaptive solution. We believe that it is attractive for an accurate study of shock/boundary-layer interaction problems in the following two aspects. First, it is naturally anisotropic so that the grid is only refined in the direction where the solution activity is high. This is particularly important for an efficient adaptive solution of the flowfield where the gradients depend strongly on the direction. For example, in the shock/boundary-layer interaction problems, the flow gradient is very high in the streamwise direction across the shock wave but relatively low along it. On the other hand, within the boundary layer, the gradient across the boundary layer is high but relatively low along it. In the interaction region, the gradient can be high in both directions, and a refinement in both directions is required. Second, an accurate solution of the shock/boundary-layer interaction problems depends on a good resolution of shock waves and shear layers in the flowfield. High-resolution methods based on approximate Riemann solvers, for example, Roe's and Osher's, are among those most successful. For multidimensional problems, a local one-dimensional Riemann problem is solved approximately at each cell interface. The directional dependency of the approximate Riemann solver limits the accuracy of solutions for grids not aligned with the discontinuities and other flow features. However, with grid movement adaption, the grid lines will automatically align themselves with the high-gradient flow feature lines such as shock waves and shear layers, which remedies the aforementioned difficulty.

The grid is adapted along each grid line in the streamwise and crossflow directions, respectively. For the second streamwise line upward, the orthogonality and the similarity to the previous line are applied as constraints to the solution-adapted grid point distribution through a spring analogy. As described by Catherall,[2] the stiffness of the springs along the line is proportional to the solution activity, whereas the spring perpendicular to the line acts as torsion springs. The control of orthogonality near the wall and the smoothness of the grid to avoid excessive skewness are very important for an accurate flow prediction in the turbulent boundary layer and the interaction region. After the grid adaption on all of the streamwise lines is completed, the solution on the initial grid is interpolated onto the newly generated grid as an initial solution. The flow is then solved on the new grid to its convergence. The weighting function is then updated, and the adaption is iterated. Generally, only a few iterations of adaption are required. After the streamwise adaption is completed, the crossflow grid adaption is carried out for each curve in the crossflow direction. Again the equidistribution algorithm is used with constraints for orthogonality and smoothness controls. The adaption in the boundary-layer normal direction supersedes the initially forced clustering of the grid points toward the wall and provides a more reasonable grid point distribution inside the turbulent boundary layer.

A proper weighting function needs to be chosen to measure the flow activity. For the shock/boundary-layer interaction problem, the pressure is chosen as the flow variable to monitor the solution activity in the streamwise direction. In the crossflow direction, the Mach number distribution is used for the grid adaption. To control the concentration of the adaptive grid, the maximum and minimum grid spacings are limited.

Results and Discussion

Delery[5] obtained a wealth of experimental data for turbulent transonic channel flows over a bump. Among the test cases, the most challenging one is case C, where a strong shock/turbulent boundary-layer interaction occurs resulting in a λ-shock structure and a shock induced boundary-layer separation. Surface pressure distributions show very little grid sensitivity. Generally, the overall comparison with the experimental data is quite good with all of the features captured by the computation. Whereas the computational wall pressure indicates little dependency on the grid, the computed flowfields show significant differences. Figure 1 shows part of the initial grid and the Mach number contours with 85 points in the streamwise direction and 65 points in the crossflow direction. The initial grid is generated algebraically with careful clustering of the grid points

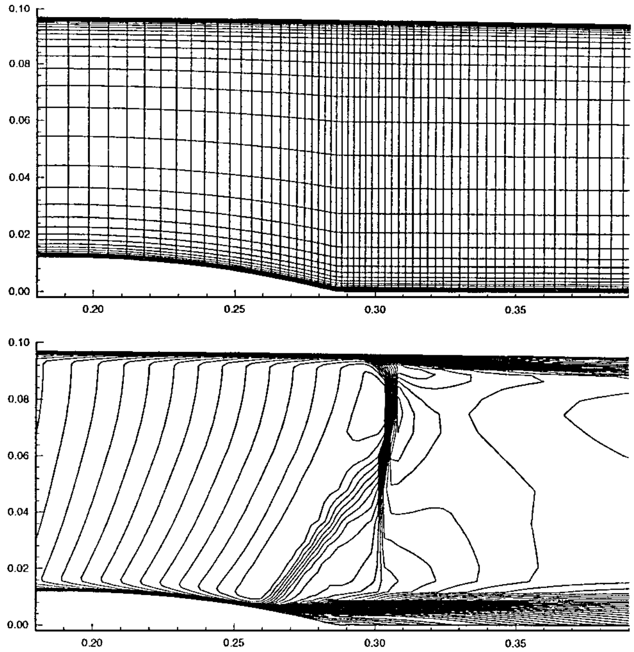

Fig. 1 Initial gird and corresponding Mach number contours.

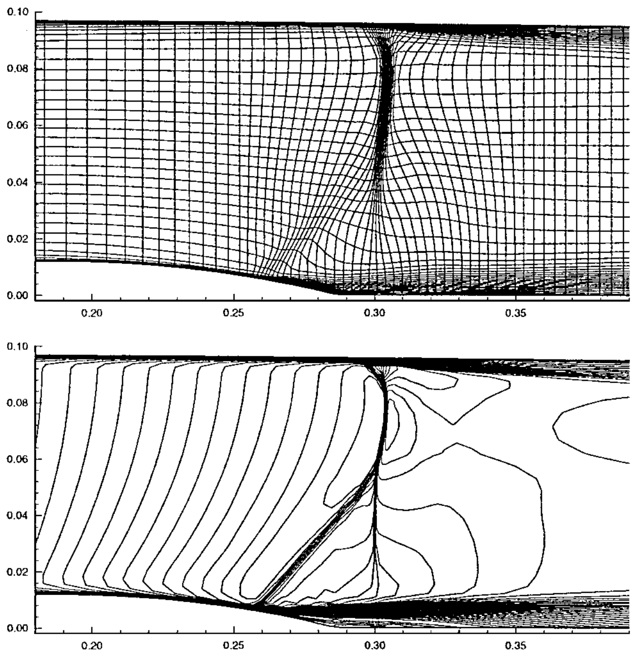

Fig. 2 Adapted gird and corresponding Mach number contours.

near the walls in the crossflow direction and around the interaction region in the streamwise direction. Adaption in both the streamwise and the crossflow directions was carried out. The adapted grid and the corresponding solution are shown in Fig. 2.

Comparing the solutions, we can clearly see the improvement of the λ-shock resolution after the grid adaption. The improvement can be seen in two aspects: 1) an improved grid density in the required direction and 2) an improved grid alignment with the flow features. The structured grid adaption has a positive effect on the alignment of the grid lines along the high gradient lines, that is, the shock waves and the shear layers. In addition to the improvement of the grid resolution normal to these lines, the alignment also improves the accuracy of the local one-dimensional approximate Riemann solver. The adaptive grid inside the boundary layer is better distributed than the initial grid, and the adaptive grid adjusts itself to trace the boundary-layer thickness. Probably more interesting is the turbulent shear stress profiles as plotted in Fig. 3. Noticeable change in the profiles for the different grids at the first two stations can be

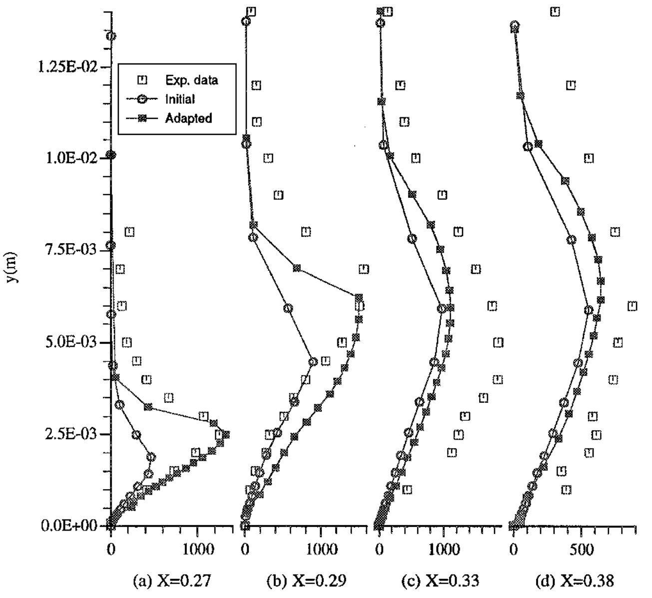

Fig. 3 Turbulence shear stress profiles for initial and adapted solutions.

observed indicating an improvement in the numerical solution with the adaptive grids.

The remaining discrepancies between the experiment and the computation, that is, the thinner separation bubble and the underprediction for turbulent shear stress after the boundary-layer reattachment, more likely come from the physical model used for the flow problem rather than from the numerical errors in the computation. The refined resolution of the λ-shock wave, both the strong oblique leg and the weak normal leg, and the boundary layer does improve the velocity and the turbulence shear stress distributions. Nevertheless, the delay in the turbulent boundary-layer recovery seems to be due to the discrepancies between the physical model used in the computation and the flow conditions in the wind-tunnel measurement.

Conclusion

To summarize, we can observe an improved prediction of the shock/boundary-layer interaction through the proposed grid adaption. This is due to 1) an improved λ-shock resolution from the streamwise grid adaption and 2) a redistribution of points inside the turbulent boundary layer from the crossflow grid adaption.

The grid alignment with the flow features makes an efficient anisotropic grid adaption possible with high grid-cell aspect ratio along both the shock wave and the boundary layer. It also alleviates the difficulty with the approximate Riemann solver, which is based on a local one-dimensional Riemann problem. For shock/turbulent boundary-layer interactions involving more complicated geometries, the structured grid adaption approach can be easily embedded in a multiblock or an overset grid strategy.

However, the grid point distribution inside the boundary layer based on Mach number distribution is not necessarily optimal, through it is better than simple stretching as demonstrated in this Note. Given a fixed number of grid points, what is the best distribution of points to resolve the turbulent boundary layer involving shock/boundary-layer interactions? The question is yet to be answered.

References

[1]Nakahashi, K., and Deiwert, G. S., "A Self-Adaptive-Grid Method with Application to Airfoil Flows," AIAA Paper 85-1525, June 1985.

[2]Catherall, D., "A Solution-Adaptive-Grid Procedure for Transonic Flows Around Aerofoils," Royal Aerospace Establishment, RAE TR 88020, Farnborough, England, UK, March 1988.

[3]Menter, F. R., "Zonal Two-Equation k–ω Turbulence Models for Aerodynamic Flows," AIAA Paper 93-2906, July 1993.

[4]Richardson, G., and Qin, N., "Linear and Non-Linear Turbulence Models for Shock-Wave/Turbulence Boundary Layer Interaction Using a Strongly Coupled Approach," AIAA Paper 98-0324, Jan. 1998.

[5]Delery, J. M., "Experimental Investigation of Turbulence Properties in Transonic Shock/Boundary-Layer Interactions," *AIAA Journal*, Vol. 21, No. 2, 1983, pp. 180–185.

J. Kallinderis
Associate Editor

Behavior of the Secondary Vortex During a Vortex-Wedge Interaction

Jin-Ho Park*
Korea Telecom Satellite Business Group, Seoul 143-190, Republic of Korea
and
Duck-Joo Lee†
Korea Advanced Institute of Science and Technology, Taejeon 305-701, Republic of Korea

I. Introduction

COHERENT vortices and their systematic interaction with downstream boundaries, especially with a leading edge, is one of the major research areas in areodynamics.[1] Ziada and Rockwell[2] have found by experiment that flowfields and surface pressure around the leading edge of a wedge are subject to significant variation by a relatively small change of the vertical distance between a wedge and incident vortices.

Recently, Park and Lee[3] numerically simulated a single vortex-wedge interaction with qualitative comparison in the experiment.[2] In Park and Lee's paper, they simulated how the incident vortex is split by the wedge, and then a secondary vortex generated from the edge of the wedge convects toward downstream, losing its vortex strength due to the viscous interaction between the secondary vortex and the boundary layer formed along the surface of the wedge.

We simulated the same single vortex-wedge interaction to investigate the behavior of the secondary vortex according to variations of an initial vertical separation distance y_v as in the experiment in Ref. 2. The adopted numerical method is the fast vortex method; the accuracy of which is detailed in Ref. 3. An incident vortex modeled by a Rankine vortex, rotating clockwise, is initially located in freestream before the wedge at the beginning of the simulation. A schematic of the vortex-wedge interaction is presented in Fig. 1. The angle of the wedge is taken as 30 deg. The Reynolds number based on freestream velocity U and the initial x position R of the incident vortex is 10^4. The R is taken as -1.0, U is 1.0, and the radius of the incident vortex H is 0.15. The lengths are nondimensionalized by R, and the time is by R/U. Calculations are carried out for the values of $y_v = 0.0$, 0.15, 0.3, and 0.375, respectively.

II. Results and Discussion

The flowfields at time $= 1.9$ for the three cases of y_v are presented in Fig. 2 via vortex particle plots, streamlines, and velocity vectors. One can see that the incident vortex is split by the wedge, and a counterclockwise rotating secondary vortex is located downstream from the edge of the wedge in each case. Figure 2 also shows that, as the y_v is higher, 1) the upper portion of the split-incident vortex increases and 2) the size of the secondary vortex increases, while 3) the velocity of the secondary vortex decreases. This tendency agrees with the experiment by Ziada and Rockwell.[2] Behaviors of the split-incident vortex in Fig. 2 are similar to the inviscid cases as

Received 15 September 1997; revision received 20 October 1998; accepted for publication 29 October 1998.

*Research Scientist, Launch Service Division, Jayang-dong 680-63, Kwangjin-gu.

†Professor, Kusung-dong 373-1, YuSung-gu. Member AIAA.